J|A|C|S
ARTICLES

Published on Web 12/08/2008

Evidence for Partially Bound States in Cooperative Molecular Recognition Interfaces

Elena Chekmeneva,[†] Christopher A. Hunter,*[,†] Martin J. Packer,[‡] and Simon M. Turega[†]

Department of Chemistry, University of Sheffield, Sheffield S3 7HF, and AstraZeneca, Alderley Park, Cheshire SK10 4TG, United Kingdom

Received May 8, 2008; E-mail: C.Hunter@sheffield.ac.uk

Abstract: A zinc porphyrin equipped with four amide H-bonding sites provides a rigid molecular receptor for the study of cooperative multipoint binding interactions. The interaction of this receptor with a variety of pyridine ligands bearing zero, one, and two H-bonding sites has been studied using UV/vis absorption, ^{1}H and ^{31}P NMR spectroscopy, and isothermal titration calorimetry in five different solvents. The results are analyzed in terms of a bound state that populates an ensemble of different complexes in which zero, one, or two of the potential H-bond interactions are formed. The key parameter that determines the behavior of the system is the product of the association constant for the H-bond interaction, K_H, and the effective molarity for the intramolecular interaction, EM. In the system reported here, EM is 0.1−1 M for all of the intramolecular interactions. For strong H-bonds (large K_H in nonpolar solvents), all of the interactions are formed in the complex and the fully bound state dominates. In this case, additional binding interactions produce incremental increases in complex stability. However, for weaker H-bonds (small K_H in polar solvents), the formation of additional interactions does not lead to an increase in the overall stability of the complex, due to the population of partially bound states.

Introduction

Multiple intermolecular interactions between two molecules in a supramolecular system usually lead to cooperative stabilization of the resulting noncovalent complex.[1−3] The magnitude of the cooperative effect can vary significantly from one system to another, but the relationship among the noncovalent interactions, the supramolecular architecture, and cooperativity is a relatively unexplored area. The field of supramolecular chemistry has been directed by the preorganization principle to rigid scaffolds and strong binding interactions that give rise to very stable complexes and readily predictable behavior[4−7] (Figure 1a). In contrast, biology works with flexible molecular frameworks and relatively weak binding interactions, relying on cooperativity between many weak interactions to organize relatively complex systems and resulting in behavior that is much more difficult to predict (Figure 1b).[8−11] All or nothing processes such as protein folding are a direct consequence of the delicate balance between the formation of a large number of weakly favorable intermolecular interactions and the restriction of a large number of conformational degrees of freedom. However, the complexity of biomolecules makes any attempt to dissect the molecular details of these processes a real challenge. In this paper, we outline an approach to the characterization of structure−cooperativity relationships in a synthetic supramolecular system.

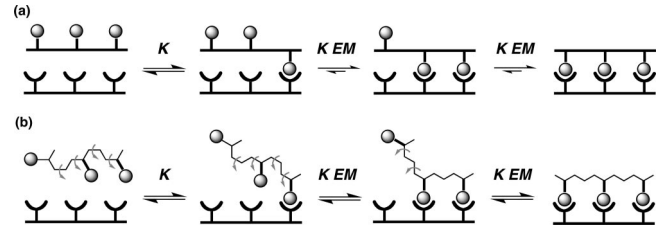

Figure 1. Cooperative binding interactions at a molecular recognition interface. (a) Systems that are highly preorganized (high EM) and/or have very favorable binding site interactions (high K) form stable well-defined complexes, where all interactions are fully made. (b) Systems that are flexible (low EM) and have weak binding site interactions (low K) have the potential to populate a large number of equilibrium states and can show dramatic cooperative responses to changes in conditions.

[†] University of Sheffield.
[‡] AstraZeneca.

(1) (a) Mulder, A.; Huskens, J.; Reinhoudt, D. N. *Org. Biomol. Chem.* **2004**, *2*, 3409–3424. (b) Philp, D.; Stoddart, J. F. *Angew. Chem., Int. Ed.* **1996**, *35*, 1155–1196. (c) Lehn, J. M. *Angew. Chem., Int. Ed.* **1990**, *29*, 1304–1319.
(2) (a) Tobey, S. L.; Anslyn, E. V. *J. Am. Chem. Soc.* **2003**, *125*, 10963–10970. (b) Hughes, A. D.; Anslyn, E. V. *Proc. Natl. Acad. Sci. U.S.A.* **2007**, *104*, 6538–6543.
(3) Jadhav, V. D.; Schmidtchen, F. P. *Org. Lett.* **2006**, *8*, 2329–2332.
(4) Mammen, M.; Choi, S. K.; Whitesides, G. M. *Angew. Chem., Int. Ed.* **1998**, *37*, 2755–2794.
(5) Hilser, V. J.; Garcia-Moreno, B.; Oas, T. G.; Kapp, G.; Whitten, S. T. *Chem. Rev.* **2006**, *106*, 1545–1558.
(6) Williams, D. H.; Bardsley, B. *Angew. Chem., Int. Ed.* **1999**, *38*, 1173–1193.
(7) Munoz, V.; Ghirlando, R.; Blanco, F. J.; Jas, G. S.; Hofrichter, J.; Eaton, W. A. *Biochemistry* **2006**, *45*, 7023–7035.
(8) Cockroft, S. L.; Hunter, C. A. *Chem. Soc. Rev.* **2007**, *36*, 172–188.
(9) Hunter, C. A.; Tomas, S. *Chem. Biol.* **2003**, *10*, 1023–1032.
(10) Shiozawa, H.; Chia, B. C. S.; Davies, N. L.; Zerella, R.; Williams, D. H. *J. Am. Chem. Soc.* **2002**, *124*, 3914–3919.
(11) Williams, D. H.; Stephens, E.; O'Brien, D. P.; Zhou, M. *Angew. Chem., Int. Ed.* **2004**, *43*, 6596–6616.

10.1021/ja803434z CCC: $40.75

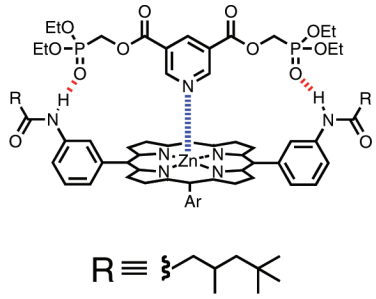

Figure 2. Supramolecular recognition interface with one metal−ligand interaction and two peripheral H-bonds.

The key parameter that quantifies the magnitude of cooperativity in a supramolecular complex is the effective molarity for the intramolecular interaction (EM). The magnitude of the EM depends on the flexibility of the linker between two binding sites and the degree of conformational strain introduced on cyclization. This relationship has been thoroughly characterized for the formation of intramolecular covalent bonds using both kinetic and thermodynamic measurements of EM.[12−14] We might assume that noncovalent interactions will show similar behavior; i.e., the EM will decrease with increasing conformational flexibility and with increasing conformational strain.[15,16] However, noncovalent interactions are much looser and conformationally less demanding than covalent bonds, which could lead to important differences in behavior.

The system illustrated in Figure 2 was designed to quantify cooperativity at a relatively complicated but tractable molecular recognition interface. The porphyrin receptor provides a rigid scaffold on which a set of binding sites can be displayed: a metal−ligand binding site and four H-bonding sites.[17,18] Zinc porphyrins are generally five-coordinate in solution and so have a single coordination site available for complexation of one pyridine ligand. The zinc porphyrin−pyridine coordination bond provides a strong noncovalent interaction site that can be used to guarantee the formation of a complex with a well-defined topology. Formation of this interaction can be easily monitored using ^{1}H NMR, UV/vis absorption, or fluorescence spectroscopy across a wide range of concentrations and solvents. The weaker H-bonding sites provide up to four additional interactions. In this study, we have varied the number of H-bonds and tuned the strength of the individual binding interactions by changing the polarity of the solvent.[19,20] The degree of flexibility in the linker that connects the coordination site and H-bond sites is another key parameter, and the conformational flexibility of the linkers used in this study leads to rather more complicated

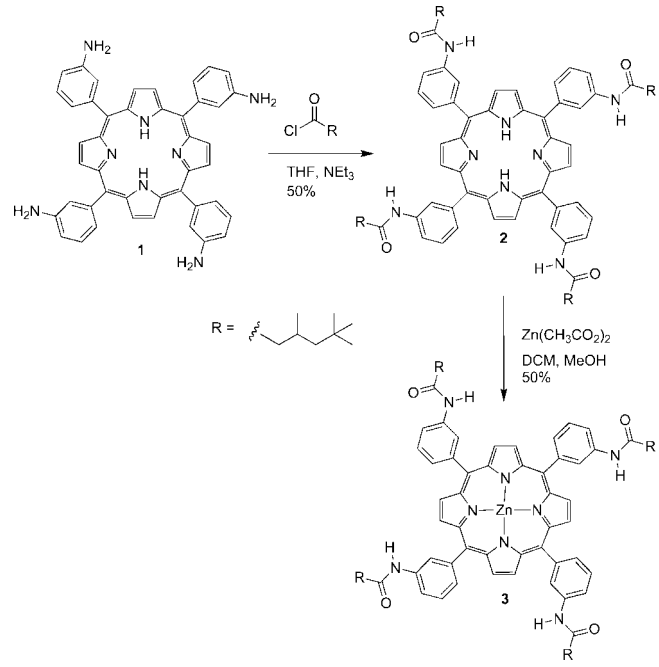

Figure 3. Synthesis of porphyrin **3**.

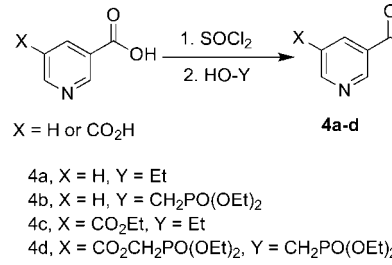

Figure 4. Synthesis of ligands **4a**−**d**.

complexation equilibria than usually observed in conventional supramolecular assemblies.

Results

The tetraamidoporphyrin used in this study was synthesized using 5,10,15,20-tetrakis(3-aminophenyl)-21*H*,23*H*-porphyrin (**1**) as a starting material (Figure 3).[21] Porphyrin **1** was coupled with isononyl chloride to provide porphyrin **2** in 50% yield. Porphyrin **2** was then metalated with zinc acetate in 50% yield to give porphyrin **3**. A set of complementary pyridine ligands containing peripheral H-bond acceptors were synthesized from the corresponding pyridine carboxylic acids (Figure 4). The pyridine carboxylic acids were first converted to the acid chloride and then coupled with the appropriate alcohol to generate ligands **4a**−**d**. Two additional control compounds, amide **5** and phosphatodiester **6**, were used to study the properties of the amide−phosphatodiester H-bond. Compound **6** is commercially available, and **5** was prepared as shown in Figure 5.

Binding of ligands **4a**−**d** to porphyrin **3** was investigated in five solvents, toluene, 1,1,2,2-tetrachloroethane (TCE), dichloromethane (DCM), chloroform, and acetone, using UV/vis absorption spectroscopy and where possible ^{1}H NMR spectroscopy, ^{31}P NMR spectroscopy, and isothermal titration calorim-

(12) Bruice, T. C.; Lightstone, F. C. *Acc. Chem. Res.* **1999**, *32*, 127–136.
(13) Cacciapaglia, R.; Di Stefano, S.; Mandolini, L. *Acc. Chem. Res.* **2004**, *37*, 113–122.
(14) Kirby, A. *Adv. Phys. Org. Chem.* **1980**, *17*, 183.
(15) Camara-Campos, A.; Hunter, C. A.; Tomas, S. *Proc. Natl. Acad. Sci. U.S.A.* **2006**, *103*, 3034–3038.
(16) Chi, X. L.; Guerin, A. J.; Haycock, R. A.; Hunter, C. A.; Sarson, L. D. *Chem. Commun.* **1995**, 2563–2565.
(17) Aoyama, Y.; Asakawa, M.; Yamagishi, A.; Toi, H.; Ogoshi, H. *J. Am. Chem. Soc.* **1990**, *112*, 3145–3151.
(18) Aoyama, Y.; Asakawa, M.; Matsui, Y.; Ogoshi, H. *J. Am. Chem. Soc.* **1991**, *113*, 6233–6240.
(19) Cook, J. L.; Hunter, C. A.; Low, C. M. R.; Perez-Velasco, A.; Vinter, J. G. *Angew. Chem., Int. Ed.* **2007**, *46*, 3706–3709.
(20) Hunter, C. A. *Angew. Chem., Int. Ed.* **2004**, *43*, 5310–5324.
(21) Semeikin, A. S.; Koifman, O. I.; Berezin, B. D. *Izv. Vyssh. Uchebn. Zaved., Khim. Khim. Tekhnol.* **1985**, *28*, 47–51.

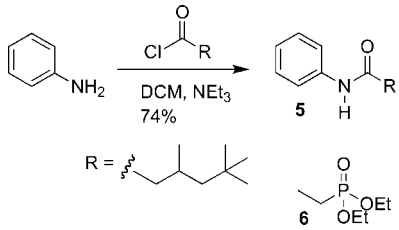

Figure 5. Synthesis of control compound **5**. Control compound **6** is commercially available.

Table 1. Association Constants (M^{-1}) for the Formation of 1:1 Complexes at 298 K[a]

solvent	**3·4a**	**3·4b**	**3·4c**	**3·4d**	method
toluene	1900	28000	850	240000	UV/vis
TCE	1600	6000	400	2500	UV/vis
TCE	940	2000	310	1700	ITC[b]
DCM	2000	11000	1200	10000	UV/vis
$CHCl_3$	1000	2300	800	3200	UV/vis
$CHCl_3$	790	2400	970	3200	ITC[b]
acetone	250	1400	120	360	UV/vis
acetone	240	1400	120	180	^{1}H NMR

[a] The average percentage error over the data set is ±30%. [b] The ^{1}H NMR spectra are broad in $CDCl_3$ and TCE, which is indicative of aggregation, so these data are considered less reliable than the UV/vis results.

etry. UV/vis absorption spectroscopy dilution experiments were first used to investigate self-association of porphyrin receptor **3**.[22−24] In the micromolar concentration range in all five solvents, the absorbance is linear with concentration, and there is no change in the wavelength of the Soret band. Thus, at these concentrations, there are no complications associated with self-interaction of the receptor. Receptor **3** is soluble at the millimolar concentrations required for NMR and isothermal titration calorimetry (ITC) experiments in TCE, chloroform, and acetone. However, the ^{1}H NMR spectrum is very broad in chloroform, indicating significant aggregation in this solvent at these concentrations (see the Supporting Information). Binding of ligands **4a**−**d** to porphyrin **3** was investigated using titrations in five solvents, toluene, TCE, DCM, chloroform, and acetone, using UV/vis absorption spectroscopy and where possible ^{1}H NMR spectroscopy, ^{31}P NMR spectroscopy, and ITC. The association constants were determined by fitting the titration data to a 1:1 binding isotherm, and there were no indications of the formation of any higher stoichiometry complexes (Table 1).

The association constants for the H-bonded **5·6** control complex were determined using ^{1}H and ^{31}P NMR titrations (Table 2), but the values are close to the limit of the range accessible in NMR titration experiments, because saturation cannot be achieved. The magnitude of association constants for simple H-bonded complexes of this type can be estimated using eq 1 as described in ref 20, where α and β are the H-bond donor and acceptor parameters of the solutes, and α_s and β_s are the corresponding parameters for the solvent.

$$\Delta G = -(\alpha - \alpha_s)(\beta - \beta_s) + 6 \text{ kJ mol}^{-1} \quad (1)$$

Table 2 compares the experimental estimates of the **5·6** association constant obtained from the NMR titrations with the theoretical estimates based on eq 1 using $\alpha = 2.9$ for the amide and $\beta = 8.9$ for the phosphatodiester. The agreement between the two sets of values gives us some confidence that the values are reasonable, despite our inability to access the full binding isotherm.

Table 2. Association Constants (M^{-1}) for the Formation of the **5·6** Complex at 298 K

solvent	α_s	β_s	$K_{eq\,1}$	K_{exptl}[a]
toluene	1.0	2.2	16	24
TCE	1.9	1.1	2.1	2.9
DCM	1.9	1.1	2.1	1.7
$CHCl_3$	2.2	0.8	0.87	0.46
acetone	1.5	5.8	0.51	1.3

[a] Measured using ^{1}H NMR or ^{31}P NMR spectroscopy. The average percentage error over the data set is ±40%.

The possibility of oxygen metal coordination makes it necessary to consider an alternative mode of cooperative binding between porphyrin **3** and ligands **4b** and **4d**. This alternative mode of binding would involve the oxygen of the phosphatodiester coordinating to the zinc of **3** and the pyridine nitrogen forming a peripheral H-bond with the amide of the porphyrin. Phosphine oxide coordination to zinc porphyrins has been observed, but with association constants of 24−32 M^{-1} in chloroform,[25] which is more than an order of magnitude lower than the corresponding pyridine−zinc porphyrin association constant. Nevertheless, it is possible to directly test the magnitude of the oxygen−zinc interaction in the system described here by titrating porphyrin **3** with control compound **6** using UV/vis absorption spectroscopy to monitor binding. The data fit well to a 1:1 binding isotherm with an association constant of 94 ± 10 M^{-1} in DCM, which is an order of magnitude lower than the pyridine−zinc association constant in this solvent (2000 M^{-1}). We can therefore rule out any significant oxygen−zinc interaction, and the coordination bonds and the H-bonds are effectively orthogonal in this system.

Spectroscopic evidence for the formation of H-bonds in the complexes can be obtained from limiting complexation-induced changes in chemical shift in the ^{1}H NMR titrations. At the concentrations required for NMR experiments (mM), the ^{1}H NMR spectrum of **3** is very broad in chloroform, which is indicative of aggregation. However, the ^{1}H NMR spectrum of **3** in acetone is much sharper, suggesting that the H-bonding solvent is able to break up amide−amide H-bonding interactions that lead to aggregation in chloroform. The limiting complexation-induced changes in chemical shift obtained from titration experiments in acetone show some interesting behavior. The amide region of the ^{1}H NMR spectra of mixtures of **3** and ligands **4a**−**d** is shown in Figure 7. Addition of **4a** or **4c** to **3** does not affect the amide signal, because these ligands do not form H-bonds. In contrast, large changes are observed on addition of **4b** or **4d**. There are large downfield shifts that are characteristic of the formation of H-bonding interactions with the phosphatodiester groups of the ligands. In addition, the singlet observed for **3** splits into several broad nonequivalent signals in the presence of the H-bonding ligands. Rotation around the porphyrin *meso*-phenyl group bonds is slow on the ^{1}H NMR time scale at room temperature, and receptor **3** therefore exists as a mixture of four different atropisomers (Figure 6). In the absence of a H-bonding ligand, the chemical

(22) Kobuke, Y.; Miyaji, H. *J. Am. Chem. Soc.* **1994**, *116*, 4111–4112.
(23) Maeda, C.; Yamaguchi, S.; Ikeda, C.; Shinokubo, H.; Osuka, A. *Org. Lett.* **2008**, *10*, 549–552.
(24) Stibrany, R. T.; Vasudevan, J.; Knapp, S.; Potenza, J. A.; Emge, T.; Schugar, H. J. *J. Am. Chem. Soc.* **1996**, *118*, 3980–3981.
(25) Officer, D. L.; Lodato, F.; Jolley, K. W. *Inorg. Chem.* **2007**, *46*, 4781–4783.

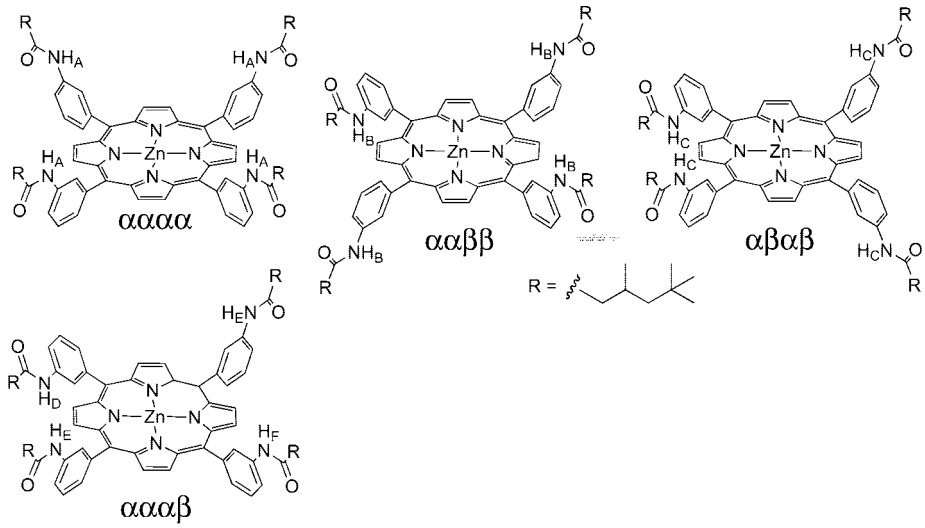

Figure 6. Atropoisomers of **3**. For a statistical equilibrium distribution, the relative populations are expected to be αααα, αα$\beta\beta$, αβαβ, and αααβ in a ratio of 1:2:1:4, which gives the relative intensities for the six amide signals A−F shown above (cf. Figure 7).

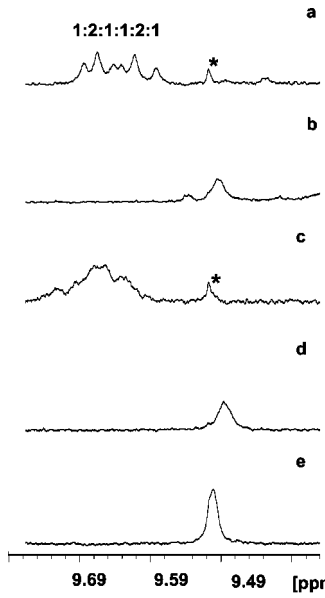

Figure 7. Amide region of the 400 MHz ^{1}H NMR spectra of porphyrin **3** in acetone-d_6: (a) **3·4d** complex, (b) **3·4c** complex, (c) **3·4b** complex, (d) **3·4a** complex, (e) unbound **3**. In all cases, the porphyrin is greater than 60% bound. There is a minor porphyrin impurity at 9.52 ppm (*) that is unaffected by the presence of ligands.

shifts of all of the amide protons in all of these isomers are similar, so a simple singlet is observed. The H-bond interactions with the phosphatodiester groups change this, so that all of the nonequivalent signals in each atropisomer are resolved in the ^{1}H NMR spectrum of the **3·4d** complex (Figure 7).

The magnitude of the average limiting complexation-induced change in chemical shift of the amide protons provides a measure of the extent of H-bonding in the porphyrin−ligand complexes (Table 3).[26,27] The 1.1 ppm increase in chemical shift observed for the **5·6** control complex corresponds to the formation of one phosphatodiester−amide H-bond. The limiting complexation-induced changes in chemical shift observed for complexes of **3·4b** and **3·4d** are about a quarter of this value, which implies that on average in both porphyrin ligand complexes only one of the four amide groups makes a H-bond with the ligand.

Table 3. Average Limiting Complexation-Induced Changes in ^{1}H NMR Chemical Shift (ppm) for the Signal due to the **3** Amide Proton on Formation of 1:1 Complexes in Acetone-d_6 at 298 K

	3·4a	**3·4b**	**3·4c**	**3·4d**	**5·6**
$\Delta\partial$	−0.03	0.27	−0.02	0.22	1.11

Table 4. Thermodynamic Data (kJ mol^{-1}) Obtained from ITC of Porphyrin **3** and Ligands **4a**−**4d** in TCE at 298 K[a]

ligand	ΔG	ΔH	$(-)T\Delta S$	$\Delta\Delta H$
4a	−17.0	−20.6	3.6	
4b	−18.8	−25.6	6.8	−5.0
4c	−14.2	−19.5	5.3	
4d	−18.4	−30.8	12.4	−11.3

[a] Average errors (kJ mol^{-1}) are ±1 in ΔG, ±1 in ΔH, and ±2 in $T\Delta S$.

Calorimetry was used to obtain further evidence for the extent of H-bonding in the complexes. ITC experiments were carried out for the complexes of porphyrin **3** and ligands **4a**−**d** in TCE. The solubility of **3** is too low to carry out the corresponding experiments in toluene, there is significant aggregation in chloroform, and the volatility of DCM and acetone makes calorimetry in these solvents unreliable. The thermodynamic parameters obtained from the ITC experiments are shown in Table 4. The magnitude of the observed enthalpy changes provides evidence for the extent to which potential binding interactions are realized in the complexes. Specifically, comparison of the values of ΔH for the control ligands **4a** and **4c** with the corresponding functional ligands **4b** and **4d** provides a measure of the extent of H-bond formation with the phosphatodiester ligands (eq 2). The results suggest that H-bonds are formed in all of the complexes that contain phosphatodiester groups, and the very large enthalpy change observed for the **3·4d** complex in TCE indicates the formation of two H-bonds in this complex.

(26) Hunter, C. A.; Packer, M. J. *Chem.—Eur. J.* **1999**, *5*, 1891–1897.
(27) Packer, M. J.; Zonta, C.; Hunter, C. A. *J. Magn. Reson.* **2003**, *162*, 102–112.

$$\Delta\Delta H_{\text{H-bond}} = \Delta H_{\mathbf{4b/d}} - \Delta H_{\mathbf{4a/c}} \quad (2)$$

Discussion

The spectroscopic data indicate that, in all cases, the pyridine ligands coordinate to the zinc center of the porphyrin, and the ligands equipped with phosphatodiester groups form H-bonds with the amide groups around the porphyrin periphery. However, the thermodynamic properties of these interactions vary significantly with solvent. The ITC experiments suggest that the **3·4d** complex forms two H-bonds in TCE, but the NMR chemical shift data in acetone suggest that on average only one of these H-bonds is formed. Thus, both the number and the strength of the binding interactions vary with the solvent. To interpret the experimental data, it will therefore be important to consider the properties of partially bound states; i.e., the bound complex in these systems must be treated as an ensemble of complexes, where only subsets of all potential binding interactions that are available are simultaneously populated. These species are illustrated in Figure 8. The overall association constant that is observed is given by the Boltzmann-weighted average of all partially bound states present in the complex. We ignore the possibility of complexes in which the metal−ligand coordination bond is broken, as this interaction is an order of magnitude more stable than the H-bonds. In addition, any degeneracy associated with complexation to one of two faces of the porphyrin is included in K_0 and is identical for all of the complexes.

We consider a stepwise binding model[28−30] with formation of a metal−ligand interaction, K_0, followed by the formation of one H-bond, K_1, and then the second, K_2. The association constant for the **3·4b** complex is given by

$$K_{\text{obsd}} = K_0\frac{1+K_1^{\,2}}{1+K_1} \quad (3)$$

where the control complex **3·4a** is used to estimate K_0.

The pyridine ligand in **4d** has an additional substituent, so the value of K_0 is different for the **3·4d** complex. Thus, using the control complex **3·4c** to estimate K_0, the association constant for the **3·4d** complex is given by

$$K_{\text{obsd}} = K_0\frac{1+K_1^{\,2}+K_1^{\,2}K_2^{\,2}}{1+K_1+K_1K_2} \quad (4)$$

The influence of solvent on the individual binding interactions can be estimated from the properties of the control complexes **3·4a**, **3·4c**, and **5·6** that feature single-point interactions (K_0 and K_H). These data can in turn be used to estimate effective molarities (EMs) for the intramolecular binding interactions in the complexes that contain cooperative multipoint contacts (Figure 8). However, if the bound state is an ensemble of different complexes, analysis of the EM values is not straightforward. For example, the value of EM for the intramolecular H-bond in the **3·4b** complex would conventionally be given by

$$\text{EM}_1 = \frac{K_{\text{obsd}}}{4K_0K_{\text{H}}} \quad (5)$$

where K_{obsd} is the observed association constant for the **3·4b** complex, K_H is the association constant for the control complex **5·6**, K_0 is the association constant for the control complex **3·4a**, and the statistical factor reflects the fact that there are four degenerate amide binding sites where H-bonds can be formed on the porphyrin.

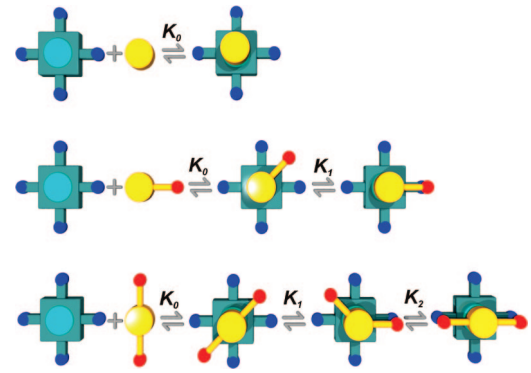

Figure 8. Sequential binding scheme for the formation of singly and doubly H-bonded complexes.

Table 5. Effective Molarities, EMs (M), and Sequential Equilibrium Constants for H-Bond Interactions, K_1 and K_2 (M^{-1}), in the Complexes Formed between Porphyrin **3** and Ligands **4b** and **4d** at 298 K[a]

	3·4b		3·4d	
solvent	K_1	EM_1	K_2	EM_2
toluene	16	0.2	10	0.5
TCE	4	0.4	0.5	0.2
DCM	6	0.8		
$CHCl_3$	3	1		
acetone	6	1		

[a] Errors: EM_1, ±60%; K_1, ±40%; EM_2, ±80%; K_2, ±60%.

However, the observed association constant is perturbed by population of the non-H-bonded state and so is not a true reflection of the stability of the complex in which both the H-bond and the coordination interaction are made simultaneously. If we take the partially bound state into account using eq 3, then a more accurate value can be obtained for the EM in this system:

$$\text{EM}_1 = \frac{K_1}{4K_{\text{H}}} = \frac{K_{\text{obsd}}}{4K_0K_{\text{H}}}\left(\frac{1+\sqrt{1+4(K_0/K_{\text{obsd}})(1-K_0/K_{\text{obsd}})}}{2}\right) \quad (6)$$

where K_{obsd} is the observed association constant for the **3·4b** complex, K_H is the association constant for the control complex **5·6**, and K_0 is the association constant for the control complex **3·4a**.

The results obtained for K_1 and EM_1 for the **3·4b** complex are presented in Table 5. The EM values are in the range 0.1−1 M, and in all cases, $K_1 > 1$, so the H-bonded complex is the dominant species in the bound state. The population of the H-bonded complex is highest in toluene (95%), where the H-bonding interactions are strongest. The maximum population of the partially bound state where the H-bond is not made is about 30% in chloroform and TCE. It is important to note that the population of the partially bound state depends on both the strength of the binding interaction, K_H, and the effective molarity, EM. In chloroform, there is a significant population of partially bound state due to solvent competition that weakens the H-bond interaction, but in TCE, a low EM leads to a similar population of partially bound state despite a stronger H-bond.

(28) Heitmann, L. M.; Taylor, A. B.; Hart, P. J.; Urbach, A. R. *J. Am. Chem. Soc.* **2006**, *128*, 12574–12581.
(29) Rodriguez-Docampo, Z.; Pascu, S. I.; Kubik, S.; Otto, S. *J. Am. Chem. Soc.* **2006**, *128*, 11206–11210.
(30) Jencks, W. P. *Proc. Natl. Acad. Sci. U.S.A.* **1981**, *78*, 4046–4050.

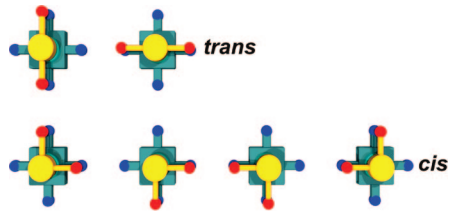

Figure 9. Two *trans* and four *cis* modes of binding in the doubly H-bonded **3·4d** complex.

If we assume that the EM_1 values measured for the **3·4b** complex can be used to estimate the stability of the singly H-bonded state in the **3·4d** complex, then the partially bound state analysis can be extended to the **3·4d** complex. The equilibrium constant between the bound state in which no H-bonds are made and the bound state in which one H-bond is made in the **3·4d** complex is given by

$$K_1 = 8(EM_1)K_H \quad (7)$$

because ligand **4d** has twice as many H-bonding sites as ligand **4b**.

Thus, combining eqs 4, 6, and 7 with the value of EM_1 determined from the **3·4b** complex, it is possible to determine EM_2 for the formation of the second H-bond in the **3·4d** complex:

$$EM_2 = \frac{8K_2}{6K_H} = \frac{8K_{obsd}}{6K_0K_H} \times \left(\frac{1+\sqrt{1+4(K_0/K_{obsd})\{1+K_1-(K_0/K_{obsd})(1+K_1^2)\}}}{2}\right) \quad (8)$$

where K_{obsd} is the observed association constant for the **3·4d** complex, K_H is the association constant for the control complex **5·6**, K_0 is the association constant for the control complex **3·4c**, and the statistical factor reflects the degeneracies of the free (8) and bound (6) states.

There are eight degenerate states for the singly H-bonded complex, because there are four amide H-bond donors on the porphyrin and two phosphatodiester H-bond acceptors on the ligand. Assumptions about the structure of the complex are required to estimate the number of degenerate states in the doubly H-bonded complex. If we assume that the two H-bonds can be formed using any pair of *meso*-amide substituents on the porphyrin, the statistical factor is 6 (Figure 9). However, if there were a strong preference for interaction with *meso* substituents that are *trans* across the face of the porphyrin, the statistical factor would be 2 (Figure 9). Similarly, if there were a strong preference for interaction with *meso* substituents that are *cis* across the face of the porphyrin, the statistical factor would be 4. This would affect the numerical results but does not significantly affect the substance of the analysis presented below. It is also important to reiterate that the control complex used to estimate K_0 in this system is different from that used for the **3·4b** complex, because the ligands have different substituents.

The results obtained for K_2 and EM_2 for the **3·4d** complex are presented in Table 5. The EM values are similar to those found for the **3·4b** complexes, between 0.1 and 1 M. However, eq 8 only has a real solution for the results obtained in toluene and TCE. This implies that two H-bonds are not formed to any significant extent in the other solvents and that the **3·4d** complexes formed in DCM, chloroform, and acetone exist as a mixture of the non-H-bonded and predominantly singly H-bonded complexes. If we assume a fixed value of EM in all systems (0.5 M), we can estimate the expected values of the observed association constants for formation of complexes in which both or only one H-bond can be made using eqs 3 and 4. Table 6 shows the results along with the relevant populations of partially bound states. For toluene and TCE, the doubly H-bonded complex is more stable than the singly H-bonded complex, but the opposite is true in the other three solvents. In other words, in DCM, chloroform, and acetone, there is nothing to be gained by forming the second H-bond, and the population of the doubly H-bonded state is correspondingly low in these solvents. The H-bonding interactions in toluene and TCE are stronger than in the other more polar solvents, so it is only in these two solvents that the gain in interaction energy is sufficient to offset the entropic organization energy required to generate the fully bound, doubly H-bonded complex. The structural evidence that supports this analysis is the ITC results that indicate the formation of two H-bonds in TCE and the NMR data that indicate the formation of only one of the two H-bonds in acetone.

Table 6. Estimated Overall Association Constants for Complexes Formed between Porphyrin **3** and Ligand **4d** That Make Either One or Two H-Bonds (M^{-1}) and Populations (%) of Partially Bound States Assuming $EM_1 = EM_2 = 0.5$ M

	singly H-bonded complex			doubly H-bonded complex			
solvent	K_{est}	zero H-bonds	one H-bond	K_{est}	zero H-bonds	one H-bond	two H-bonds
toluene	8.2×10^4	1	99	6.8×10^5	0	10	90
TCE	3.3×10^3	8	92	3.6×10^3	4	46	50
DCM	7.1×10^3	13	87	6.4×10^3	8	56	35
$CHCl_3$	1.2×10^3	35	65	1.1×10^3	32	58	10
acetone	5.6×10^2	16	84	4.9×10^2	11	59	29

Conclusions

In complexes that make multiple intermolecular interactions, partially bound states, where not all of the individual binding sites are simultaneously populated, can make a significant contribution to the behavior of the system.[31−33] There is a balance between the favorable free energy change associated with formation of an individual interaction and the free energy penalty associated with formation of a more organized complex. The organization energy is quantified by the effective molarity (EM) for the intramolecular binding interaction, and the free energy contribution associated with formation of an individual binding interaction can be estimated from the association constants of model reference complexes where only one binding interaction is made (K). Thus, the product K(EM) is the key parameter that dictates the extent to which cooperative multipoint binding interactions are made in a particular system. We assume that the free energy contributions of individual binding interactions are approximately constant, additive, and independent of their context, provided that the interaction is fully made and there are no significant secondary interactions.[34]

In the experiments presented here, we have used a porphyrin−ligand system that can form up to three noncovalent intermolecular binding interactions: a metal−ligand coordination in-

(31) Williams, D. H.; Davies, N. L.; Koivisto, J. J. *J. Am. Chem. Soc.* **2004**, *126*, 14267–14272.
(32) Calderone, C. T.; Williams, D. H. *J. Am. Chem. Soc.* **2001**, *123*, 6262–6267.
(33) Williams, D. H.; Davies, N. L.; Zerella, R.; Bardsley, B. *J. Am. Chem. Soc.* **2004**, *126*, 2042–2049.

teraction that is so favorable that it can be assumed to be fully bound in all situations ($K = 100-2000$ M^{-1})[35,36] and two weaker H-bonding interactions ($K = 0.5-25$ M^{-1}). The H-bonding sites are connected via moderately flexible linkers giving effective molarities in the 0.1−1 M range; i.e., there is a small unfavorable organization energy associated with the formation of an intramolecular H-bond that reduces the effective molarity from 10 M, which is the value expected on the basis of estimates of the cost of restricting intermolecular motion.[20] Although there is some variation in the measured effective molarities reported here, the results are rather similar for all of the complexes and do not differ significantly, given the experimental error.

The free energy contribution associated with formation of intramolecular H-bonds was varied by tuning the polarity of the solvent. In toluene, there is very little solvent competition, so there is a large driving force for the formation of a H-bond ($K = 24$ M^{-1}). In this solvent, K(EM) ≈ 10, so that the fully bound complex is formed in which all three binding sites are fully populated (>90% occupancy of bound states). In this case, a simple increase in stability is observed for each interaction that is added to the system: when the ligand cannot make any H-bonds, $K \approx 10^3$ M^{-1}, for a ligand that can make one H-bond, $K \approx 10^4$ M^{-1}, and for a ligand that can make two H-bonds, $K \approx 10^5$ M^{-1}.

The behavior in the more polar solvents is more complicated. Here K(EM) ≈ 1, so that the system is delicately balanced and the probability of formation of an intramolecular H-bond is 50:50. In these solvents, complexes that could potentially form zero, one, or two H-bonds all have rather similar overall stability constants, and a detailed dissection of all of the small contributions that affect the association constants is required to interpret the results. The individual H-bonding interactions are most favorable in TCE ($K = 3$ M^{-1}), and in this solvent, there is clear evidence from ITC experiments for the formation of two intramolecular H-bonds in the bound state. In other words, the K(EM) balance is tipped in favor of the fully bound, doubly H-bonded state by K in this case. However, detailed analysis of the thermodynamic properties of this complex suggests a significant population of partially bound states in which only one H-bond is made (40%), and no increase in the overall stability of the complex is observed. For this system, although the spectroscopic data clearly show that H-bonds are made, this does not lead to any significant increase in the association constant as the number of H-bonding groups increases. In the other three solvents, DCM, chloroform, and acetone, K(EM) < 1, due to increased solvent competition with the H-bonding interactions, and there is no evidence for significant population of the doubly H-bonded complex. However, ^{1}H NMR spectroscopy shows that on average one of the porphyrin amides forms a H-bond with the ligand in acetone, and detailed analysis of the thermodynamic properties of these complexes indicates that the major species present in the bound state is the singly H-bonded complex (60%). This complex in which only one of the two H-bonds is formed enjoys an 8-fold degeneracy relative to the bound state in which no H-bonds are made, and this provides an additional entropic stabilization of the H-bond in the partially bound state.

The system described here represents a new tool for probing the properties of complicated recognition interfaces and delineating the rules that govern cooperativity in molecular interactions. The expression of individual binding site interactions in the overall stability of a complex is determined by the relationship between the binding site interaction strength, K, and the effective molarity, EM, and the relationship between these parameters, the chemical structure, and the supramolecular architecture should be a fruitful area for further investigation. Systems that are poised at the balance point of K(EM) ≈ 1 are a hallmark of biological organization and recognition, and not only will synthetic counterparts prove useful in understanding the molecular basis for the properties of such systems, they may also exhibit functionally related behavior.

Experimental Section

Synthesis. 5,10,15,20-Tetrakis(3,5,5-trimethyl-*N*-phen-3-ylhexanamide)-21*H*,23*H*-porphine, 2. To a mixture of **1** (0.325 g, 0.482 mmol) and triethylamine (1.63 mL, 11.6 mmol) in THF (20 mL) under nitrogen at room temperature was added isononanoyl chloride (0.366 mL, 1.93 mmol), and the solution was stirred for 18 h. The solution was concentrated under reduced pressure and the resulting blue gum dissolved in DCM (250 mL), washed with 10% $NaHCO_3$(aq) (2 × 200 mL) and brine (200 mL), and condensed under reduced pressure. The crude product was purified on silica (30 g) eluting with DCM/5% methanol. The product **2** was isolated as a purple solid: yield 0.297 g (50%); mp 250 °C dec; ^{1}H NMR (250 MHz, CD_3SOCD_3) $\delta_H = 10.25$ (1H, s), 8.89 (2H, s), 8.50 (1H, d, $J = 10$ Hz), 8.08 (1H, s), 7.92 (1H, d, $J = 8$ Hz), 7.74 (1H, dd, $J = 8$ Hz, $J = 8$ Hz), 2.39−2.2 (2H, m), 2.19 (1H, s), 1.36−1.06 (2H, m), 0.98 (3H, d, $J = 5$ Hz), 0.88 (9H, s), −2.96 (0.5H, s); MS (EI+) m/z (rel intens) = 675 (100), 1236 (10) [M + H$^+$]; HRMS (EI+) m/z calcd for $C_{80}H_{99}N_8O_4$ 1235.7789, found 1235.7825; UV/vis (DMSO) λ_{max}/nm (ε/mol^{-1} cm^{-1}) 423 (5.1×10^5), 516 (1.8×10^4), 551 (7.9×10^3), 590 (5.3×10^3), 645 (4.2×10^3).

5,10,15,20-Tetrakis(3,5,5-trimethyl-*N*-phen-3-ylhexanamide)porphine zinc(II), 3. A mixture of **2** (0.300 g, 0.243 mmol) and zinc acetate (0.890 g, 4.85 mmol) in chloroform (20 mL)/MeOH (30 mL) was stirred under nitrogen at room temperature for 1.5 h. The solution was concentrated under reduced pressure, and the resulting blue gum was purified on deactivated alumina (80 g) eluting with DCM. The product **3** was isolated as a purple solid: yield 0.159 g (50%); mp 195 °C dec; ^{1}H NMR (250 MHz, $CDCl_3$, CD_3OD 2%) $\delta_H = 8.89$ (2H, s), 8.76 (1H, s), 8.19−8.14 (1H, m), 8.00−7.86 (2H, m), 7.57 (1H, s), 2.38−2.28 (2H, m), 2.14−2.04 (1H, m), 1.28−1.02 (2H, m), 0.96 (3H, d, $J = 5$ Hz), 0.83 (9H, s); MS (EI+) m/z (rel intens) = 1299 (100) [M$^+$]; HRMS (EI+) m/z calcd for $C_{80}H_{96}N_8O_4{}^{64}Zn$ 1296.6846, found 1296.6835; UV/vis (DMSO) λ_{max}/nm (ε/mol^{-1} cm^{-1}) 421 (4.6×10^5), 549 (1.6×10^4), 595 (4.7×10^3).

(Diethoxyphosphoryl)methyl Nicotinate, 4b. A mixture of nicotinic acid (1 g, 8.12 mmol), toluene (10 mL), DMF (10 μL), and $SOCl_2$ (15 mL) was refluxed for 1 h under protection by a DryRite drying tube. The solution was condensed under reduced pressure, and DCM (120 mL) was added. Then diethyl hydroxymethyl phosphonate (1.20 mL, 8.12 mmol) in DCM (20 mL) and triethylamine (3.39 mL, 24.4 mmol) were added in small portions. The solution was allowed to stir for 18 h, then washed with $NaHCO_3$(aq) (2 × 100 mL) and brine (100 mL), dried with $NaSO_4$, and condensed under reduced pressure. The crude product was purified on silica (25 g) eluting with EtOAc containing 0.25% triethylamine. The product was isolated as a clear oil: yield 2.71 g (98%); ^{1}H NMR (250 MHz, $CDCl_3$) δ_H 9.19 (d, 1H, $J = 2$ Hz), 8.75 (dd, 1H, $J = 2, 5$ Hz), 8.26 (dt, 1H, $J = 2, 8$ Hz), 7.35 (m,

(34) We assume that there is no cooperativity (positive or negative) associated with changes in the intrinsic affinity of the metal−ligand or H-bond interactions (K_0 and K_H) on formation of multiple intermolecular contacts in these systems: Ercolani, G. *J. Am. Chem. Soc.* **2003**, *125*, 16097–16103.

(35) Dattagupta, N.; Malakar, D.; Ramcharan, R. G. *J. Inorg. Nucl. Chem.* **1981**, *43*, 2079–2080.

(36) Zielenkiewicz, W.; Lebedeva, N. S.; Antina, E. V.; Vyugin, A. I.; Kaminski, M. *J. Solution Chem.* **1998**, *27*, 879–886.

1H), 4.59 (d, 2H, $J = 9$ Hz), 4.16 (dq, 4H, $J = 7$, 14 Hz), 1.30 (t, 6H, $J = 7$ Hz); ^{13}C NMR (62.9 MHz, $CDCl_3$) $\delta_C = 164.42$ (d, $J =$ 8 Hz), 153.97, 151.08, 137.33, 125.24, 123.48, 62.97 (d, $J = 6$ Hz), 57.58 (d, $J = 170$ Hz), 16.51 (d, $J = 6$); MS (EI+) *m/z* (rel intens) = 274 (40) [M + H$^+$], 547 (100) [2M + H$^+$], 569 (60) [2M + Na$^+$]; HRMS (EI+) *m/z* calcd for $C_{11}H_{17}NO_5P$ 274.0844, found 274.0857; FT-IR (thin film) ν_{max}/cm^{-1} 2982, 2934, 1736, 1593, 1423, 1329, 1275, 1249, 1119, 1052, 1025, 971.

Diethyl Pyridine-3,5-dicarboxylate, 4c. A mixture of 3,5-pyridinedicarboxylic acid (1 g, 5.98 mmol), toluene (10 mL), DMF (15 μL), and $SOCl_2$ (30 mL) was refluxed for 1 h under protection by a DryRite drying tube. The solution was condensed under reduced pressure, and DCM (120 mL) was added. Then ethanol (3.50 mL, 60 mmol) in DCM (20 mL) and triethylamine (6.78 mL, 48.8 mmol) were added in small portions. The solution was allowed to stir for 18 h, then washed with $NaHCO_3$(aq) (2 × 100 mL) and brine (100 mL), dried with $NaSO_4$, and condensed under reduced pressure. The crude product was purified on silica (25 g) eluting with EtOAc/hexane. The product was isolated as a clear oil: yield 1.18 g (91%); ^{1}H NMR (250 MHz, $CDCl_3$) $\delta_H = 9.30$ (s, 1H), 8.79 (s, 0.5H), 4.39 (q, 2H, $J = 7.1$ Hz), 1.37 (t, 3H, $J = 7.1$ Hz); ^{13}C NMR (62.9 MHz, $CDCl_3$) $\delta_C =$ 164.45, 154.09, 137.88, 126.20, 61.80, 14.24; MS (EI+) *m/z* (rel intens) = 196 (20), 224 (100) [M + H$^+$]; HRMS (EI+) *m/z* calcd for $C_{11}H_{14}NO_4$ 244.0923, found 224.0931; FT-IR (thin film) ν_{max}/cm^{-1} 2987, 1730, 1601, 1450, 1369, 1314, 1259, 1243, 11.01, 1027.

Bis(diethoxyphosphoryl) Pyridine-3,5-dicarboxylate, 4d. A mixture of 3,5-pyridinedicarboxylic acid (1 g, 5.98 mmol), toluene (10 mL), DMF (15 μL), and $SOCl_2$ (30 mL) was refluxed for 1 h under protection by a DryRite drying tube. The solution was condensed under reduced pressure, and DCM (120 mL) was added. Then diethyl hydroxymethyl phosphonate (1.20 mL, 8.12 mmol) in DCM (20 mL) and triethylamine (6.78 mL, 48.8 mmol) were added in small portions. The solution was allowed to stir for 18 h. DCM (200 mL) was added, and the resulting solution was then washed with $NaHCO_3$(aq) (2 × 100 mL) and brine (100 mL), dried with $NaSO_4$, and condensed under reduced pressure. The crude product was purified on silica (60 g) eluting with DCM/0−5% methanol gradient. The product was isolated as a clear oil: yield 2.20 g (80%); ^{1}H NMR (250 MHz) $\delta_H = 9.36$ (d, 2H, $J = 2$ Hz), 8.85 (t, 1H, $J = 2$ Hz), 4.62 (d, 4H, $J = 9$ Hz), 4.18 (dq, 8H, $J = 7$, 8 Hz), 1.31 (t, 12H, $J = 7$ Hz); ^{13}C NMR (62.9 MHz, $CDCl_3$) $\delta_C = 163.68$ (d, $J = 8$ Hz), 154.98, 138.78, 125.54, 63.28 (d, $J = 6$ Hz), 58.18 (d, $J = 170$ Hz), 16.74 (d, $J = 6$ Hz); MS (EI+) *m/z* (rel intens) = 468 (100) [M + H$^+$], 490 (40) [M + Na$^+$]; HRMS (EI+) *m/z* calcd for $C_{17}H_{28}NO_{10}P_2$ 468.1188, found 468.1170; FT-IR (thin film) ν_{max}/cm^{-1} 2985, 2931, 1737, 1600, 1331, 1260, 1227, 1103, 1054, 1025, 971.

3,5,5-Trimethyl-*N*-phenylhexanamide, 5. A mixture of aniline (1.51 g, 16.1 mmol) and triethylamine (6.79 mL, 48.3 mmol) in DCM (125 mL) protected by a $CaCl_2$ drying tube was cooled to 0 °C. To this was added isononyl chloride (2.84 g, 16.1 mmol), and the resulting mixture was stirred for 18 h. The solution was then washed with $NaHCO_3$(aq) (2 × 100 mL) and brine (100 mL), dried with $NaSO_4$, and condensed under reduced pressure. The crude product was purified on silica (80 g) eluting with hexane/ethyl acetate. The product was isolated as a waxy solid: yield 2.79 g (74%); ^{1}H NMR (250 MHz, $CDCl_3$) $\delta_H = 8.02$ (s, 1H), 7.70 (d, 2H, $J = 8$ Hz), δ 7.44 (t, 2H, $J =$ 8 Hz), 7.24 (t, 1H, $J = 7$ Hz), 2.41 (m, 3H), 1.36 (m, 2H)1.18 (d, 3H, $J = 6$ Hz), 1.60 (s, 9H); ^{13}C NMR (62.9 MHz, $CDCl_3$) $\delta_C = 171.45$, 138.21, 129.03, 124.29, 120.25, 50.76, 47.63, 31.22, 30.16, 27.65, 22.81; MS (EI+) *m/z* (rel intens) = 234 (100) [M + H$^+$], 256 (60) [M + Na$^+$]; HRMS (EI+) *m/z* calcd for $C_{15}H_{24}NO$ 234.1858, found 234.1866; FT-IR (thin film) ν_{max}/cm^{-1} 3295, 3058, 2956, 2905, 2862, 1654, 1603 1543 1499, 1444, 1364, 1302, 1251, 1204.

UV/Vis Absorption Titrations. UV/vis titrations were carried out by preparing a 10 mL sample of the porphyrin **3** at known concentration (1−10 μM) in spectroscopic grade solvent. A 2 mL portion of this solution was removed, and a UV/vis spectrum was recorded using a Peltier thermostat set at 298 K (Table 7). A 2 mL solution of pyridine ligand (5−2000 μM) was prepared using the porphyrin solution, so that the concentration of porphyrin remained constant throughout the titration. Aliquots of pyridine solution were added successively to the cell containing the porphyrin solution, and the UV/vis spectrum was recorded after each addition. Changes in absorbance for the Soret band of the porphyrin were fit to a 1:1 binding isotherm in Microsoft Excel to obtain the association constant. Each titration was repeated at least twice, and the experimental error is quoted as 2 times the standard deviation at a precision of one significant figure.

Table 7. λ_{max} of Porphyrin **3** in the Solvents Used in This Study

	toluene	DCM	$CHCl_3$	acetone
λ_{max}/nm	425	421	420	425

UV/vis dilutions of **3** were carried out by preparing a 0.03 mM solution of porphyrin **3** in DCM. Aliquots of porphyrin **3** solution were added successively to a cell containing 2 mL of DCM, and the UV/vis spectrum was recorded after each addition. Changes in the absorbance of the Soret band fit well to a Lambert−Beer law showing no signs of aggregation.

Isothermal Titration Calorimetry. ITC experiments were performed at 25 °C on a VP-ITC MicroCal titration calorimeter (MicroCal, Inc., Northampton, MA). In a typical calorimetric measurement, porphyrin was dissolved in spectroscopic grade solvent ($CHCl_3$, $C_2H_2Cl_4$, toluene, DCM) at a concentration on the order of 0.5−1 mM, and the solution was loaded into the sample cell of the microcalorimeter. The guest solution (15−20 times more concentrated than the host solution) was loaded into the injection syringe. The number of injections was between 50 and 60, and the volumes of the injections were between 5 and 7 μL with 30−40 s of duration and 300 s of spacing between the injections. Dilution experiments were performed for each titration by loading the guest solution (at the same concentration as the titration experiment) into the injection syringe and adding the guest to pure solvent in the cell. The dilution data were subtracted from each host titration thermogram. The data fitting was performed by using ORIGIN (version 7.0, Microcal, LLC ITC) and a 1:1 binding isotherm (One Set of Sites model), fixing the stoichiometry number to 1 and allowing the stability constant K and binding enthalpy ΔH values to float. At least two independent measurements were performed for each complex, and the average results are shown.

Dilution experiments were used to check for the effects of aggregation of the porphyrin host. The porphyrin solution was loaded into the sample cell, and pure solvent was added from the syringe. In all cases, the dimerization constant and the dimerization enthalpy were too low to be measured, so aggregation can safely be ignored in these experiments.

^{1}H NMR Titrations. NMR titrations were carried out by preparing a 3 mL sample of host at known concentration (1 mM for porphyrin hosts and 50 mM for **6**). Then 0.6 mL of this solution was removed, and a ^{1}H NMR spectrum was recorded. A 2 mL solution of guest (10−1400 mM) was prepared using the host solution, so that the concentration of porphyrin remained constant throughout the titration. Aliquots of guest solution were added successively to the NMR tube containing the host, and the NMR spectrum was recorded after each addition. Changes in chemical shift for the porphyrin aromatic signals were analyzed by using the appropriate binding isotherms in Microsoft Excel. Each titration was repeated at least twice, and the experimental error is quoted as twice the standard deviation at a precision of one significant figure.

Acknowledgment. We thank the EPSRC (C.A.H. and S.M.T.) for funding.

Supporting Information Available: UV/vis absorption dilution data for **3** in all five solvents, ^{1}H NMR spectra of **3** in acetone, TCE, and chloroform, and NMR spectroscopic characterization of **2**, **3**, **4b**, **4c**, **4d**, and **5**. This material is available free of charge via the Internet at http://pubs.acs.org.

JA803434Z